Phosphorylation of the Rab exchange factor Sec2p directs a switch in regulatory binding partners

Danièle Stalder[a], Emi Mizuno-Yamasaki[a,1], Majid Ghassemian[b], and Peter J. Novick[a,2]

[a]Department of Cellular and Molecular Medicine and [b]Department of Chemistry and Biochemistry, Biomolecular and Proteomics Mass Spectrometry Facility, University of California, San Diego, La Jolla, CA 92093

This contribution is part of the special series of Inaugural Articles by members of the National Academy of Sciences elected in 2013.

Contributed by Peter J. Novick, October 24, 2013 (sent for review October 3, 2013)

Sec2p is a guanine nucleotide exchange factor that promotes exocytosis by activating the Rab GTPase Sec4p. Sec2p is highly phosphorylated, and we have explored the role of phosphorylation in the regulation of its function. We have identified three phosphosites and demonstrate that phosphorylation regulates the interaction of Sec2p with its binding partners Ypt32p, Sec15p, and phosphatidyl-inositol-4-phosphate. In its nonphosphorylated form, Sec2p binds preferentially to the upstream Rab, Ypt32p-GTP, thus forming a Rab guanine nucleotide exchange factor cascade that leads to the activation of the downstream Rab, Sec4p. The nonphosphorylated form of Sec2p also binds to the Golgi-associated phosphatidyl-inositol-4-phosphate, which works in concert with Ypt32p-GTP to recruit Sec2p to Golgi-derived secretory vesicles. In contrast, the phosphorylated form of Sec2p binds preferentially to Sec15p, a downstream effector of Sec4p and a component of the exocyst tethering complex, thus forming a positive-feedback loop that prepares the secretory vesicle for fusion with the plasma membrane. Our results suggest that the phosphorylation state of Sec2p can direct a switch in its regulatory binding partners that facilitates maturation of the secretory vesicle and helps to promote the directionality of vesicular transport.

membrane traffic | yeast | phospho-regulation | vesicle maturation

Rab GTP-binding proteins serve as key regulators of membrane traffic. They act by recruiting a wide variety of effectors that together can direct the major steps of vesicular traffic, including vesicle budding, delivery, tethering, and fusion of the vesicle with the acceptor compartment (1). They function as molecular switches that toggle from a cytosolic, inactive conformation (GDP-bound) to a membrane-associated, active conformation (GTP-bound). This fundamental characteristic enables them to recruit effectors only when associated with a specific membrane domain. Importantly, this switch is under control of guanine nucleotide exchange factors (GEFs), making these proteins critical determinants for the localization of active Rab proteins (reviewed in ref. 2).

Sec4p is a Rab protein that associates specifically with secretory vesicles traveling from the Golgi to sites of polarized growth in yeast. It plays an essential role at this stage of the secretory pathway by recruiting at least three different effectors. In its GTP-bound form, Sec4p binds directly to Myo2p, a type V myosin, on secretory vesicles, to promote their transport along polarized actin cables, to Sec15p, a component of the exocyst complex that tethers secretory vesicles to the plasma membrane in preparation for exocytic fusion, and to Sro7p, an Lgl family member shown to regulate exocytic SNARE function (3–5). The ability of Sec4p to interact with these effectors depends upon its activation by its GEF, Sec2p (6).

Sec2p is a large protein of 759 amino acids divided into several domains. The N-terminal region (amino acids 1–160) forms a long, homodimeric coiled-coil domain. Importantly, this domain contains the active site that catalyzes the Sec4p GDP-to-GTP exchange reaction (6, 7). The remainder of Sec2p interacts with a variety of other components that together control its cellular localization and thereby regulate its exchange activity. Sec2p tagged with GFP is concentrated at exocytic sites including prebud sites, the tips of small buds, and at the mother–daughter neck (8). Sec2p is brought to these sites by riding on secretory vesicles as they are delivered by the type V myosin, Myo2p, on polarized actin cables.

A key observation was that localization of Sec2p to exocytic sites requires its interaction with the Golgi-associated Rab, Ypt32p, in its GTP-bound state (9). This finding suggested the existence of a Rab GEF cascade mechanism in which one Rab, Ypt32p, in its activated state recruits Sec2p, which in turn activates the next Rab on the pathway, Sec4p. This mechanism has been conserved through evolution. A Rab GEF cascade involving the corresponding mammalian homologs Rab11–Rabin8–Rab8 has been shown to coordinate ciliogenesis, impairment of which has been implicated in numerous genetic disorders (10). Other examples of Rab GEF cascades have been reported, establishing the widespread use of a mechanism that likely ensures both continuity and directionality in membrane traffic pathways (reviewed in ref. 11; 12, 13).

Sec2p also serves as a key component in another important regulatory circuit. Sec2p binds directly to Sec15p, an effector of Sec4p and a subunit of the exocyst-tethering complex (14). The formation of this GEF/Rab/effector complex potentially constitutes a positive-feedback loop that could lead to the creation of a membrane microdomain marked by a high concentration of Sec4-GTP and exocyst complex. Importantly, the Sec15p-binding site in Sec2p overlaps with the Ypt32p-binding site just downstream of the catalytic domain (amino acids 160–258), and Sec15p and Ypt32p compete against each other for binding to

Significance

Rab proteins control and coordinate the various biochemical reactions involved in membrane traffic. We investigate the role of phosphorylation in the regulation of Sec2p, an exchange protein that activates the Rab controlling the final stage of the secretory pathway. We show that phosphorylation directs a switch in the regulatory circuitry involving Sec2p that leads to maturation of the vesicles in preparation for fusion with the plasma membrane. This complex regulatory mechanism has been conserved from yeast to animal cells where it is used to direct the assembly of the cilium, a structure on the cell surface needed for cell signaling and the loss of which underlies a number of human diseases.

Author contributions: D.S., E.M.-Y., and P.J.N. designed research; D.S., E.M.-Y., and M.G. performed research; D.S., E.M.-Y., M.G., and P.J.N. analyzed data; and D.S. and P.J.N. wrote the paper.

The authors declare no conflict of interest.

[1]Present address: Institute for Molecular and Cellular Regulation, Gunma University, 3-39-15 Showa-machi, Maebashi 371-8512, Japan.

[2]To whom correspondence should be addressed. E-mail: pnovick@ucsd.edu.

This article contains supporting information online at www.pnas.org/lookup/suppl/doi:10.1073/pnas.1320029110/-/DCSupplemental.

Sec2p (14). The implication is that Sec2p can be involved in either a GEF cascade or a GEF–effector positive-feedback loop but not both at the same time. A downstream region (amino acids 450–508) negatively regulates the binding of Sec15p to Sec2p by an auto-inhibitory mechanism. Truncation or point mutations within this domain lead to increased binding to Sec15p, and limited proteolysis analysis suggests that these Sec2p mutants are in a more accessible, open, conformation (14).

Recently, we found that the phosphoinositide phosphatidylinositol-4-phosphate [PI(4)P] plays an important role in regulating the association of Sec2p with its alternate binding partners, Ypt32-GTP and Sec15p (15). PI(4)P is highly enriched on Golgi membranes and works in concert with Ypt32p-GTP to recruit Sec2p onto Golgi-derived vesicles by interacting with Sec2p through three positively charged patches. Interestingly, the interaction with PI(4)P keeps Sec2p in an auto-inhibited conformation that prevents its association with Sec15p on nascent secretory vesicles. However, the level of PI(4)P appears to drop before the secretory vesicles are concentrated at exocytic sites. This drop in PI(4)P concentration relieves the auto-inhibition, allowing a switch in Sec2p binding partners from Ypt32p to Sec15p and results in the formation of the Sec2p/Sec4p/Sec15p GEF–effector complex that promotes tethering of the vesicle to the plasma membrane in preparation for exocytic fusion.

Several studies have suggested that, after vesicle tethering, Sec2p must be released from the exocyst complex so that it will be available to engage in additional rounds of vesicular traffic (8, 14). Sec2p mutants that are not auto-inhibited by the 58-amino acid domain cannot recycle and, even in their cytosolic form, remain bound to Sec15p. The nature of the signal that normally triggers the release of Sec2p from Sec15p has not yet been addressed.

Previously, we have shown that Sec2p is highly phosphorylated in vivo (8). Here we explore the role of phosphorylation in the regulation of Sec2p function. In this study, we identify previously unknown phosphosites within the Sec15p/Ypt32p-GTP–binding region of Sec2p. We show that phosphorylation promotes the interaction of Sec2p with Sec15p and inhibits binding to Ypt32p-GTP and PI(4)P. Our findings suggest that Sec2p must cycle between a phosphorylated and a nonphosphorylated state for optimal localization and efficient vesicular transport. We propose that Sec2p is phosphorylated as secretory vesicles mature to promote its interaction with the exocyst complex. Then, the vesicle is tethered to the plasma membrane, Sec2p is dephosphorylated and released into the cytoplasm to facilitate new rounds of vesicular transport.

Results

Phosphorylation of Sec2p Increases Binding to the Exocyst Component Sec15p. We have explored a possible regulatory role for phosphorylation in the interaction of Sec2p with Sec15p. GST-tagged Sec2p was isolated from bacterial or yeast lysates using glutathione beads. Yeast Sec2p was then treated with calf intestinal phosphatase (CIP) (Fig. 1). Note that untreated yeast Sec2p has a reduced electrophoretic mobility compared with bacterial Sec2p or yeast Sec2p dephosphorylated by CIP treatment. Thus, in a yeast lysate Sec2p is predominantly phosphorylated. The GST-Sec2p samples were then used in binding assays with purified, recombinant, hexahistidine (His_6)-tagged full-length Sec15p. The amount of Sec15p bound was evaluated by immunoblot using an anti-Sec15p antibody. Phosphorylated Sec2p isolated from yeast showed a fourfold increase in Sec15p binding relative to Sec2p isolated from bacteria or CIP-treated yeast Sec2p.

Phosphosites at the C Terminus of Sec2p Do Not Regulate Its Interaction with Known Binding Partners. According to the phosphoGRID (www.phosphogrid.org/) and PhosphoPep databases (www.sbeams.org/devDC/sbeams/cgi/Glycopeptide/peptideSearch.cgi), Sec2p can be phosphorylated near its C terminus on serines 515, 524, 544, and

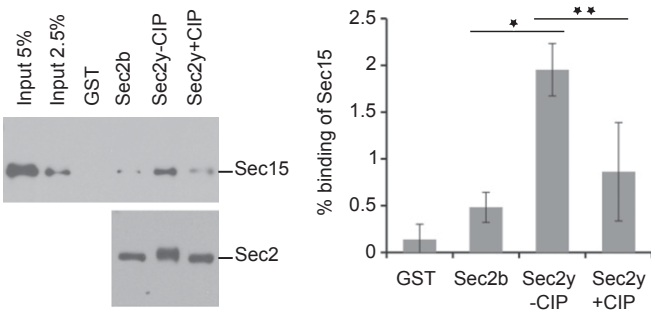

Fig. 1. Phosphorylation of Sec2p increases binding to the exocyst component Sec15p in vitro. (*Left*) GST-Sec2p was purified from bacteria (Sec2b) or from yeast (Sec2y). Sec2y was treated with the phosphatase CIP or was left untreated. His_6-Sec15p was purified from bacteria, eluted, and incubated with GST-Sec2p immobilized on glutathione beads. Bound Sec15p was detected with anti-Sec15p antibody, and GST-Sec2p was detected with anti-GST antibody. (*Right*) The percentage of bound Sec15p was calculated and is indicated. The mean and SD of three different experiments are shown. $*P < 0.002$; $**P < 0.05$, Student *t* test.

545. To evaluate the importance of these phosphosites, all four of these serines were mutated either to alanines, to block phosphorylation (Sec2p M13), or to aspartates, to mimic the phosphorylated state (Sec2p M14). We explored whether these Sec2p mutants were altered in their interactions with any of the known Sec2p binding partners. Using in vitro binding assays with recombinant proteins, we evaluated the interaction of Sec2p M13 and M14 with Sec15p and Ypt32p-GTP (Fig. S1*A*). We also used sedimentation analysis to assess the interaction of the Sec2p mutants with liposomes containing PI(4)P (Fig. S1*B*). As shown in Fig. S1, Sec2p M13 and M14 were not affected in their interaction with Sec15p, Ypt32p, or PI(4)P. Together, these results indicate that phosphorylation of Sec2p at its C terminus does not regulate the interaction of Sec2p with any of the known Sec2p binding partners. Therefore, the dephosphorylation of these sites could not account for the effect of CIP treatment on the Sec2p–Sec15p interaction (Fig. 1). This result implies that there must be additional sites of phosphorylation.

Identification of Phosphosites Within the Binding Region for Sec15p/Ypt32p. In an earlier study (8) we observed that Sec2p truncated at amino acid 508 was labeled in vivo with ^{32}P-orthophosphate to a similar extent as full-length Sec2p, indicating that phosphosites must exist in addition to serines 515, 524, 544, and 545. To identify these sites, we performed mass spectrometry on GST-Sec2p 1-508 purified from yeast. Four phosphosites were identified: S181, S186, S188, and S200 (Fig. 2 and Fig. S2). Interestingly, serines 181, 186, and 188 lie within a large serine/threonine patch of seven residues, and alignment of Sec2p with its mammalian homolog, Rabin8, shows that this patch is close to the $STSS^{243}$ stretch that very recently has been shown to be subject to phosphorylation in Rabin8 (Fig. 2*B*) (16, 17). This general region of Sec2p is involved in binding to both Ypt32p-GTP and Sec15p. For this reason, these three phosphorylation sites were analyzed further.

To confirm these findings, we investigated the mobility of nonphosphorylatable and phosphomimetic Sec2p-mutant alleles in which all possible phosphosites between residues 181 and 188 were mutated respectively to alanines or to aspartates/glutamates (S to D and T to E). As mentioned above, wild-type Sec2p purified from yeast showed a reduced electrophoretic mobility compared with a sample treated with the phosphatase CIP (Fig. 1, *Left* and Fig. 2*C*). However, the nonphosphorylatable Sec2 mutant showed only a slight difference in electrophoretic mobility compared with the CIP-treated control, suggesting that this Sec2p mutant is less highly phosphorylated (Fig. 2*C*). In contrast,

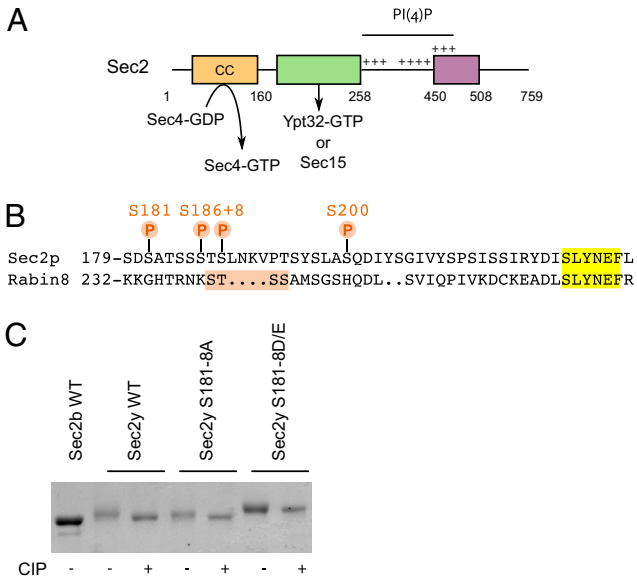

Fig. 2. Identification of three previously unknown phosphosites in the Sec15p/Ypt32p-binding region. (*A*) Domain organization of Sec2p. The N-terminal region contains a coiled-coil domain (CC) that catalyzes the exchange of GDP for GTP on Sec4p. Just downstream, are overlapping binding sites for Sec15p and Ypt32p-GTP, which compete against each other to bind to Sec2p. Three positively charged patches allow Sec2p to interact directly with the phosphoinositide PI(4)P. Finally, the region from amino acid 450–508 negatively regulates Sec15p binding to Sec2p by an auto-inhibitory mechanism. (*B*) Alignment (by Lalign, www.ch.embnet.org/software/LALIGN_form.html) of the sequence containing the serines 181, 186, and 188 with the mammalian homolog Rabin8. (*C*) The phosphorylation-dependent mobility shift of the nonphosphorylatable Sec2p mutant S181–8A and the phosphomimetic Sec2p mutant S181–8D/E. GST-tagged Sec2p was purified from bacteria (Sec2b) or from yeast (Sec2y) and was treated with the phosphatase CIP or was left untreated. Sec2 proteins were visualized by Coomassie Brilliant Blue staining after SDS/PAGE.

the phosphomimetic Sec2p mutant had a reduced mobility which was almost completely insensitive to CIP treatment. These results suggest that the major in vivo phosphosites of Sec2p lie between residues 181 and 188.

Phosphomimetic Sec2 Mutants Display Increased Binding for Sec15p in Vitro and in Vivo. To explore further if phosphorylation regulates the interaction of Sec2p with the exocyst component Sec15p, we generated phospho-mutants in which S181, S186, or S188 was mutated to alanine, preventing phosphorylation, or to aspartate, as phosphomimetic alleles. We expressed these GST-tagged proteins in bacteria, purified them, and used them in binding assays with purified, recombinant His_6-tagged full-length Sec15p (Fig. 3, *Upper*). We found that neither the S-to-A nor the S-to-D mutations at position 181 affected the interaction of Sec2p with Sec15p (Fig. 3*A*). However, we observed that phosphomimetic Sec2p mutants at both positions 186 and 188 exhibited increased binding to Sec15p (Fig. 3 *B* and *C*). A similar result was obtained with a Sec2p phosphomimetic allele in which the entire S/T patch (S181–S188) was mutated (S to D and T to E) (Fig. 4*A*, *Upper*). These observations further support a role for phosphorylation in promoting the interaction of Sec2p with the exocyst component Sec15p.

To test the effects of the phosphosite-mutations on the interaction of Sec2p with Sec15p in a more physiological condition, we investigated the coprecipitation efficiency of Sec15p-13×myc with Sec2p-3×GFP from lysates of yeast expressing both tagged proteins as the sole copy and at endogenous levels. Immunoprecipitation of Sec2p-3×GFP with anti-GFP antibody was performed on total lysates. These immunoprecipitates were then probed with anti-myc antibody to detect Sec15p. As shown in Fig. 4*B*, significantly more Sec15p-13×myc was coprecipitated with the phosphomimetic Sec2p mutant S181–8D/E than with wild-type Sec2p or with a nonphosphorylatable allele of Sec2p.

Phosphomimetic Sec2 Mutants Display Decreased Binding of Ypt32p-GTP. The Sec2p phospho-mutants next were tested to see if their affinity for Ypt32p-GTP was affected. We used His_6-tagged, full-length, recombinant Ypt32p preloaded with GTPγS and performed in vitro binding assays. The amount of bound Ypt32p-GTP was evaluated by immunoblot using an anti-Ypt32p antibody (Fig. 3 *B* and *C* and Fig. 4*A*, *Lower*). We observed an inverse correlation between Sec15p binding and Ypt32p-GTP binding. The phosphomimetic Sec2p mutants (S186D, S188D, and S181–8D/E) exhibited decreased binding of Ypt32p-GTP. This result indicates that phosphorylation not only increases the affinity of Sec2p for the exocyst component Sec15p but also inhibits the binding to Ypt32p-GTP. Because Sec15p and Ypt32p compete against each other in binding to Sec2p, the net effect of Sec2p phosphorylation would be a shift from Ypt32p binding to Sec15p binding.

Phosphomimetic Sec2 Mutant Inhibits Binding to PI(4)P. Next, we explored the effects of the phospho-mutations on the interaction of Sec2p with the phosphoinositide PI(4)P. We incubated wild-type, the nonphosphorylatable, and the phosphomimetic Sec2p mutants (S181–8A and S181–8D/E respectively) with sucrose-loaded liposomes containing 5% PI(4)P or control liposomes. The Sec2p-KA mutant, previously shown to be defective in PI(4)P binding (15), was used as a negative control. Liposome-bound Sec2p was precipitated by centrifugation and detected by Coomassie blue staining. Although the nonphosphorylatable Sec2p mutant showed no difference in PI(4)P binding relative to the wild-type Sec2 protein, the phosphomimetic Sec2p mutant displayed significantly reduced affinity for the phosphoinositide, dropping from 77% binding to about 54% (Fig. 5). Thus, phosphorylation of Sec2p inhibits binding to both the phosphoinositide PI(4)P and to Ypt32p-GTP. Because PI(4)P inhibits the Sec2p–Sec15p interaction, the reduced affinity of phosphorylated Sec2p for PI(4)P could further promote the binding of Sec2p to Sec15p.

Phosphorylation Does Not Induce a Change in Sec2p Conformation Detectable by Partial Proteolysis. Several Sec2p mutants, such as Sec2-78p or Sec2-M7, were shown in prior studies to bind more efficiently than wild-type Sec2p to Sec15p (14, 15). These mutants also exhibited a different limited proteolysis pattern when subjected to trypsin digestion, suggesting that these mutants are in an alternate, more accessible, conformation. Because phosphorylated yeast Sec2p and the phosphomimetic Sec2p S181–8D/E mutant show increased binding of Sec15p, we examined the pattern of trypsin digestion of these proteins. GST-tagged wild-type or mutant Sec2 proteins were purified from bacteria or from yeast, were treated with the phosphatase CIP or were left untreated, and then were incubated with trypsin. The pattern of digestion products was detected with anti-Sec2 antibody (Fig. S3). Wild-type Sec2p showed a major degradation product of 70 kDa, whereas Sec2p-M7, used as a control for the alternate conformation, was degraded more rapidly and showed a major degradation product of 50 kDa. Surprisingly, all other Sec2 alleles tested, including phosphorylated yeast Sec2p and the phosphomimetic Sec2p mutant, had a degradation pattern similar to wild-type Sec2p. These results suggest that, although phosphorylation leads to increased Sec15p binding, it does not trigger a major conformation change in Sec2p that is detectable by this method.

Blocking the Sec2 Phospho-Cycle Affects Sec2 Localization and Growth. To study the importance of Sec2p phosphorylation in vivo, we introduced different phospho-mutations into the *SEC2*

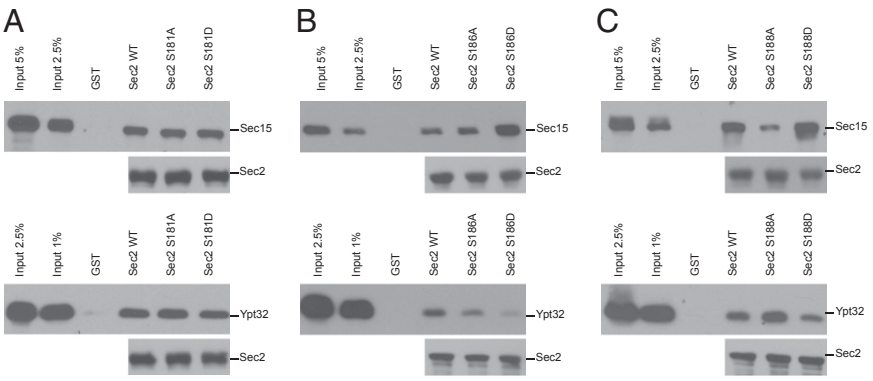

Fig. 3. Phosphomimetic mutation of serines 186 and 188, but not 181, leads to increased binding of Sec15p and a corresponding decrease in binding of Ypt32p-GTP. (*A–C*) GST-Sec2p, His_6-Sec15p, and His_6-Ypt32p were purified from bacteria. Sec15p and Ypt32p were eluted. Ypt32p was preloaded with GTPγs and then was incubated with GST-Sec2p immobilized on glutathione beads. Bound proteins were detected with anti-Sec15p antibody or anti-Ypt32p antibody. GST-Sec2 was detected with anti-GST antibody.

locus and fused the 3×GFP sequence to the C terminus. Even when we mutated all residues of the S/T patch from S181 to S188, neither the phosphomimetic nor the nonphosphorylatable Sec2p mutants showed a growth defect at any temperature, and the localization of the Sec2 mutant proteins appeared normal (Fig. S4 *A* and *B*). Therefore, we investigated whether there were any synthetic effects when the Sec2p phospho-mutations were introduced into a sensitized genetic background. We used a yeast strain carrying two mutations, *ypt31Δ* and $ypt32^{A141D}$, that together lead to a loss of the redundant functions of Ypt31p and Ypt32p. Diploids carrying the nonphosphorylatable or the phosphomimetic Sec2 alleles (S181–8A and S181–8D/E, respectively) in addition to the *ypt31Δ* $ypt32^{A141D}$ alleles were sporulated, and the tetrads were dissected at 25 °C. Spores carrying only the *ypt31Δ* $ypt32^{A141D}$ alleles grew normally at 16 °C, 25 °C, 30 °C, and 32 °C but exhibited temperature-sensitive growth at 37 °C, as previously reported (18) (Fig. 6 *A* and *B*). In contrast, spores expressing either the nonphosphorylatable or the phosphomimetic Sec2 in addition to the *ypt31Δ* $ypt32^{A141D}$ alleles grew slowly at 16 °C, 25 °C, 30 °C, and 32 °C, with a more severe growth defect for the nonphosphorylatable Sec2 mutant (Fig. 6 *A* and *B*). These results suggest that blocking the Sec2p phosphocycle negatively affects Sec2p function.

Using the same approach, we tested various combinations of mutations in the S/T patch to define the minimum number of mutations that will induce a growth defect (double mutation of S186 and S188, mutation of all residues from S184–S188, and, as a control, mutation of the entire S/T patch from S181–S188). A double mutation of S186 and S188 was not sufficient to affect yeast growth even though phosphomimetic mutations at either one of these sites increased binding to Sec15p in vitro (Fig. 6*B*). Phosphomimetic mutations in Sec2p from residues S184–S188 were sufficient to induce a growth defect, whereas mutation of the entire S/T patch from S181–S188 was required for the nonphosphorylatable Sec2 alleles. These results suggest that the entire S/T patch might play a role in phospho-regulation.

Next we looked at the localization of the nonphosphorylatable and the phosphomimetic Sec2p mutants (S181–8A and S181–8D/E) in the sensitized *ypt31Δ* $ypt32^{A141D}$ background (Fig. 6*C*). In a wild-type background, Sec2p-3×GFP localized to the bud tips of small and medium-sized buds and to the mother–daughter neck of larger cells. In the *ypt31Δ* $ypt32^{A141D}$ background, localization of Sec2p-3×GFP was observed at the mother–daughter neck;

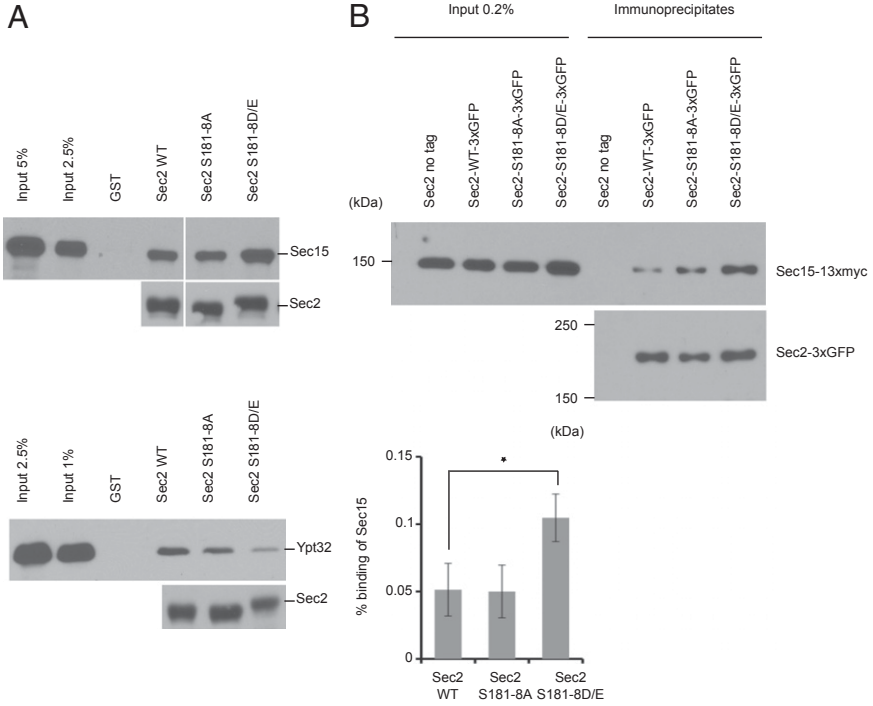

Fig. 4. A Sec2p phosphomimetic allele in which the entire S/T patch was mutated displays increased binding of Sec15p in vitro and in vivo. (*A*) In vitro binding assays, performed as in Fig. 3, of bacterial purified wild-type GST-Sec2p, S181–8A, and S181–8D/E proteins with His_6-Sec15p (*Upper*; the vertical white space indicates where intervening lanes have been removed for presentation purposes) or His_6-Ypt32p-GTPγs (*Lower*). (*B*) Phosphomimetic Sec2p mutant S181–8D/E has an enhanced interaction with Sec15p in yeast cells. Wild-type Sec2p-3×GFP, S181–8A, or S181–8D/E was immunoprecipitated with GFP antibody in yeast strains coexpressing Sec15p-13×myc (NY3047, NY3048, and NY3049, respectively). A yeast strain expressing untagged Sec2p (NY2546) was used as a negative control. Coprecipitated Sec15p-13×myc and the amount of Sec15p-13×myc in 0.2% of the lysates were detected with anti-myc antibody. The amount of Sec2p-3×GFP in the immunoprecipitates was detected with anti-GFP antibody. The intensity of the bands was quantified using ImageJ. The percentage of Sec15p bound to Sec2p was calculated and is indicated. The mean and SD of three different experiments are shown. $*P < 0.03$, Student *t* test.

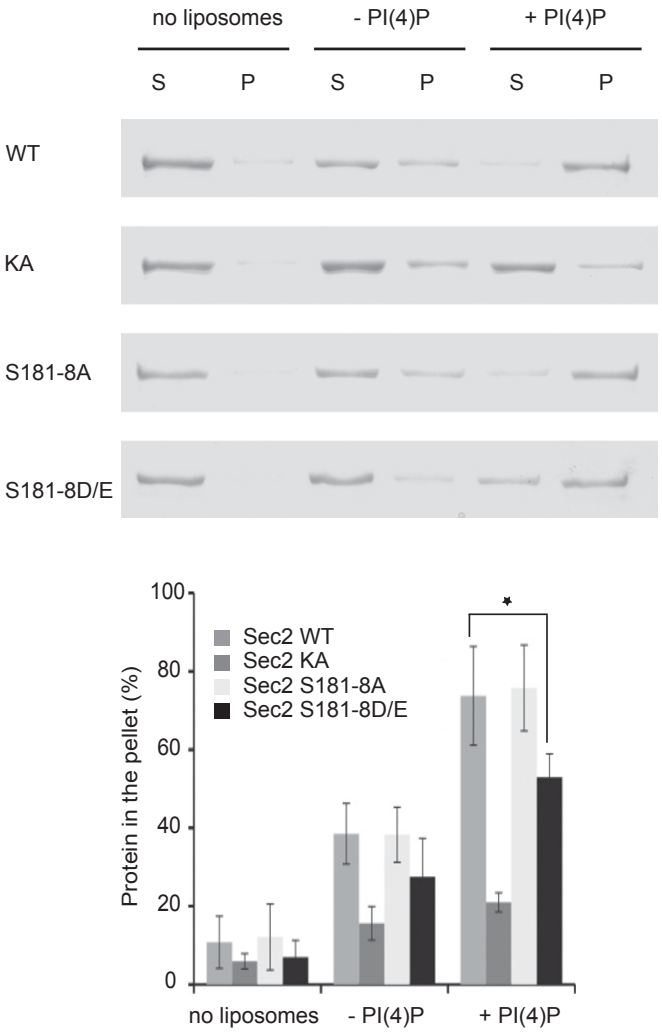

Fig. 5. Phosphomimetic Sec2 mutation inhibits binding to the phosphoinositide PI(4)P. Bacterial purified wild-type GST-Sec2p, Sec2p KA (negative control), and Sec2p with phospho-mutations (S181–8A or D/E) were incubated with liposomes containing, or not, 5 mol% PI(4)P. Liposomes were precipitated, and proteins in the supernatant (S) and in the pellet (P) were visualized by Coomassie Brilliant Blue staining after SDS/PAGE. The intensity of the bands was quantified using ImageJ. The mean and SD of three different experiments are shown. $*P < 0.05$, Student *t* test.

however, the localization to the bud tips was affected, dropping from 80% to 30% (compare Fig. S4*B* and Fig. 6*C*). The introduction of phospho-mutations into Sec2p induced an almost complete loss of the polarized localization of Sec2p at the bud tip, and the localization at the mother–daughter neck dropped from 60% to 30–40%. Again, the phenotype was more severe for the nonphosphorylatable allele than for the phosphomimetic Sec2 allele. These results indicate that blocking the Sec2 phospho-cycle affects not only yeast growth but also Sec2 localization and, taken together, suggest that full Sec2p function requires cycling between the unphosphorylated and phosphorylated states.

Nonphosphorylatable Sec2 Mutant Causes Aberrant Membrane Accumulation in a Sensitized Background. Loss-of-function mutations in *sec2*, such as *sec2-78*, cause an accumulation of secretory vesicles (6). To investigate the role of Sec2p phosphorylation in membrane traffic, the nonphosphorylatable Sec2p mutant was shifted to 32 °C for 1 h and then was examined by electron microscopy. In a wild-type background, no membrane accumulation indicative of a traffic defect was observed (Fig. S4*C*). However, a strong effect was observed in cells expressing the *sec2* S181–8A allele in a *ypt31Δ ypt32*^{A141D} background (Fig. 7). At the nonpermissive temperature (37 °C), *ypt31Δ ypt32*^{A141D} cells accumulate a large number of aberrant Golgi-related structures termed "Berkley bodies," as previously reported (18). However, at 32 °C, the *ypt31Δ ypt32*^{A141D} strain expressing wild-type Sec2p showed only a slight increase in Golgi structures, whereas the triple mutant expressing Sec2 S181–8A appeared to exacerbate the *ypt31Δ ypt32*^{A141D} phenotype. A large number of aberrant Golgi-like structures accumulated, and the yeast cells appeared swollen. This observation is consistent with an earlier report showing that a defect in the exocytic component Sec1p (*sec1-1*) also leads to the accumulation of Golgi membranes in the *ypt31Δ ypt32*^{A141D} background (18). These results indicate that phosphorylation of Sec2p is important to ensure efficient vesicular transport.

Discussion

Rab GEFs play a key role in membrane traffic, determining where and when a specific Rab protein is activated. Here we analyze the role of phosphorylation in the regulation of Sec2p, a GEF for the exocytic Rab, Sec4p. Membrane recruitment of Sec2p is mediated by its affinity for PI(4)P and Ypt32p-GTP (9, 15). These two ligands act in concert to recruit Sec2p to Golgi-derived secretory vesicles. Sec2p also interacts with Sec15p, a subunit of the exocyst complex and a direct effector of Sec4p-GTP (14). Ypt32p-GTP and Sec15p compete against each other for binding to Sec2p, suggesting that the interaction of Sec2p with these two components may be sequential. PI(4)P acts to block Sec15p binding and thereby promotes binding to Ypt32p-GTP on the late Golgi or nascent vesicles where the PI(4)P concentration is highest. However, once the vesicles concentrate at exocytic sites, the PI(4)P concentration is reduced, allowing Sec15p to replace Ypt32p on Sec2p (15). The formation of this Sec2p–Sec15p GEF–effector complex may initiate a positive-feedback loop that promotes Sec4p activation and effector recruitment and thereby prepares the vesicle for docking and fusion to the plasma membrane.

Phosphorylation serves as an important regulatory mechanism in membrane traffic; for example, the HOPS tether subunit Vps41p undergoes phosphorylation by the Yck3p kinase, and this modification directs a shift from a role in endosome–vacuole tethering to a second role in tethering AP-3 vesicles to the vacuole (19). Sec2p undergoes phosphorylation within two different regions of the protein. Phosphomimetic mutations at previously known phosphosites (serines 515, 524, 544, and 545) do not significantly affect the interaction of Sec2p with Ypt32p-GTP, PI(4)P, or Sec15p. In contrast, phosphorylation or mutation of the phosphosites identified in this study affects the interaction of Sec2p with each of its binding partners. Phosphomimetic alleles (S186D, S188D, and S181–8D/E) promote the binding of Sec2p to Sec15p and inhibit binding to both Ypt32p-GTP and PI(4)P, whereas a nonphosphorylatable allele (S181–8A) binds at a level similar to the nonphosphorylated wild-type protein. Thus, phosphorylation helps direct a shift in Sec2p function from its initial stage of membrane recruitment, driven by interactions with Ypt32p-GTP and PI(4)P, to a positive-feedback loop, involving an interaction between Sec2p and Sec15p, that is needed in preparation for exocytic fusion (Fig. 8). A reduction in PI(4)P concentration before the concentration of vesicles at exocytic sites appears to work in concert with phosphorylation to drive this shift in Sec2p function. However, the exact mechanism by which Sec2p switches from one regulatory mode to the other remains to be determined. Our limited proteolysis results suggest that phosphorylation does not trigger a major conformational change in Sec2p, unlike the mutations in the autoinhibitory region (amino acids 450–508) that promote

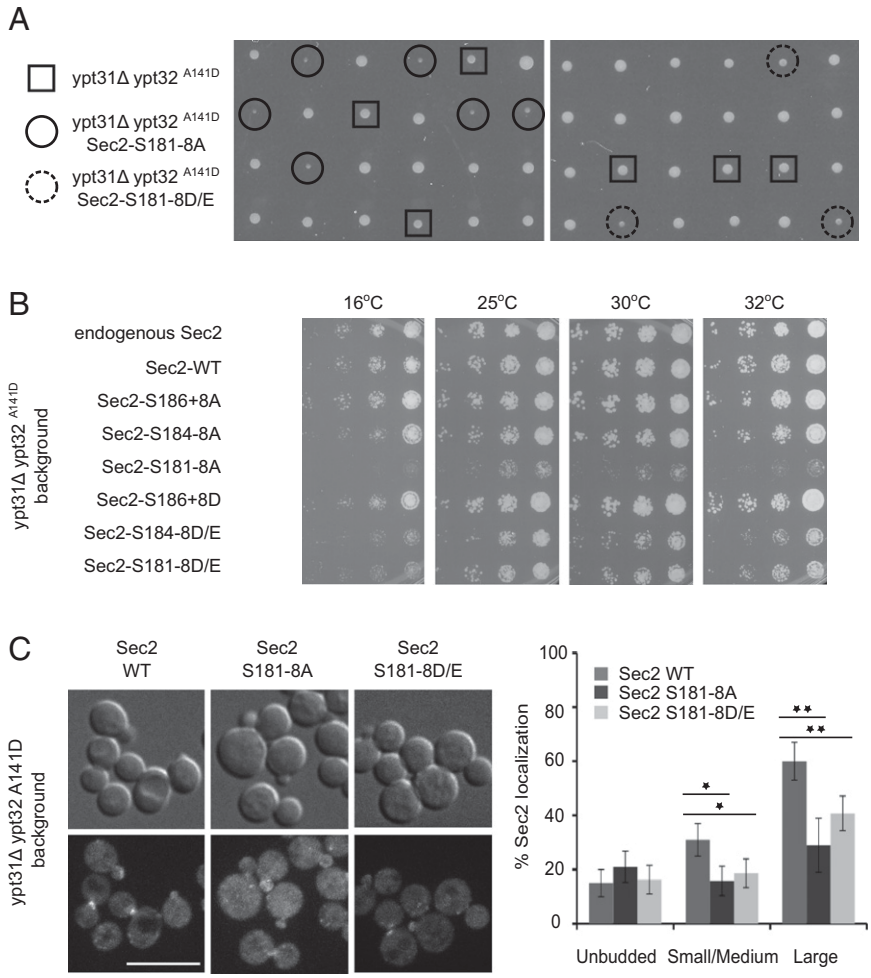

Fig. 6. Locking Sec2p in either its phosphorylated or unphosphorylated state affects both its localization and yeast growth. (*A*) Tetrads dissected from diploid strains carrying the *sec2–3×GFP S181–8A* or *D/E*, *ypt31Δ*, and *ypt32^{A141D}* alleles. *ypt31Δ* and *ypt32^{A141D}* spores are shown within squares. The triple-mutant spores *ypt31Δ* and *ypt32^{A141D} sec2p S181–8A* or *D/E* are shown within continuous or dashed circles, respectively. (*B*) Serial dilutions of cells expressing different phospho-mutant alleles of Sec2p in the *ypt31Δ ypt32^{A141D}* background. Cells were spotted and grown on YPD plates at 25 °C, 30 °C, or 32 °C for 2 d or at 16 °C 6 d. (*C*) Localization of wild-type Sec2p-3×GFP and phospho-mutants (S181–8A and D/E) fused to 3×GFP. Cells were grown overnight at 25 °C to midlog phase in a synthetic medium containing 2% glucose and then were pelleted and observed immediately. (Scale bar, 10 μm.) Around 150 cells were counted for each experiment, and the mean and SD of three different experiments are shown. Values indicate the percentage of cells showing a polarized localization of Sec2p in unbudded cells or an accumulation of Sec2p at the bud tip of small/medium cells or at the mother–daughter neck of larger cells. *$P < 0.02$; **$P < 0.005$, Student *t* test.

Sec15p binding. Phosphorylation may enhance the interaction of Sec2p with Sec15p and inhibit binding to Ypt32p-GTP and PI(4)P through more subtle changes and thereby push the reaction forward. Further structural analysis will be necessary to address this mechanism. Several studies have suggested that, after vesicle tethering, Sec2p must be released from the exocyst complex so that it can associate with a new round of secretory vesicles (8, 14). Our data show that trapping Sec2p in a phosphorylated state negatively affects its function and localization. These findings are consistent with a model in which dephosphorylation of Sec2p promotes the release of Sec2p from Sec15p after vesicle tethering.

Striking parallels exist between the regulation of the final stage of the yeast secretory pathway and the pathway leading to ciliogenesis in mammalian cells. Not only are homologs of each of the yeast components expressed in mammalian cells and required for ciliogenesis, but the complex regulatory interrelationships between these components are preserved as well. Rabin8, the homolog of Sec2p, is recruited to the pericentrosome at the base of the cilia by binding to Rab11 (10), the homolog of Ypt32p, but it also binds to the mammalian homolog of Sec15p. Interestingly, phosphorylation of Rabin8 at S272, a site that aligns with the 181–188 region of Sec2p, promotes binding to Sec15p and inhibits binding to Rab11 (16), exactly paralleling the regulation we report here. Although Rabin8 does not bind to PI(4)P, as does Sec2p, it does bind to phosphatidylserine, and this affinity is reduced by phosphorylation, just as the affinity of Sec2p for PI(4)P is reduced by phosphorylation (16).

Despite the striking parallels between the phospho-regulation of Sec2 and Rabin8, the regulatory kinases are likely to be different. Phosphorylation of Rabin8 at serine 272 is directed by the NDR2 kinase (16, 17). The yeast NDR kinase, Cbk1, binds to Sec2p and will phosphorylate Sec2p in vitro (20). Nonetheless, the phosphosites in the 181–188 region do not fit the consensus for phosphorylation by the Cbk1 kinase. Furthermore, the loss of Cbk1p function impairs the secretory pathway at a stage upstream of Sec2p action. Therefore, it is likely that the phosphorylation of Sec2p is mediated primarily by another kinase, which has yet to be identified. In *Candida albicans*, Sec2p is

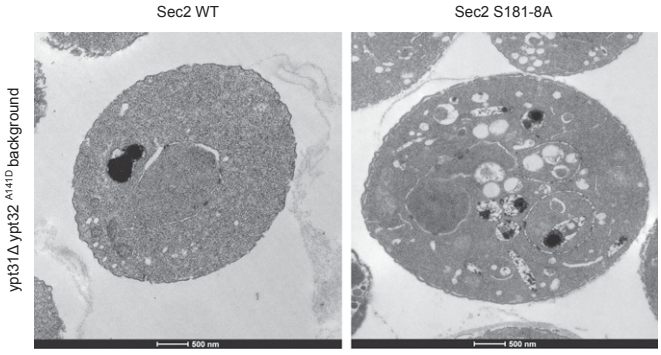

Fig. 7. A nonphosphorylatable Sec2 mutant affects vesicular export from the Golgi. Triple mutants *ypt31Δ ypt32^{A141D} sec2-3×GFP* [either wild-type (NY3040) or S181–8A (NY3045)] were shifted at midlog phase to 32 °C for 1 h and were processed for thin-section electron microscopy.

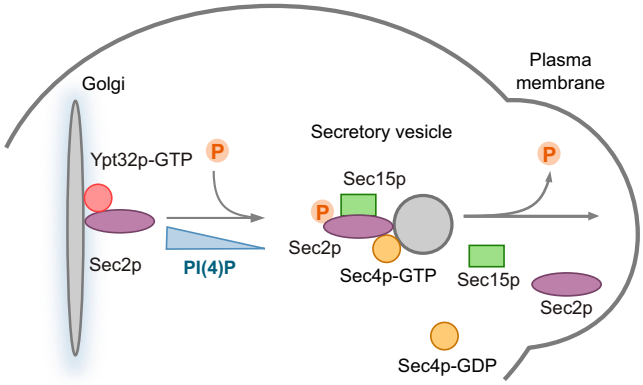

Fig. 8. A model for the Sec2p phospho-cycle in the secretory pathway. Sec2p, in its nonphosphorylated form, is recruited to the Golgi membrane by binding to both Ypt32p-GTP and PI(4)P. The Golgi-derived secretory vesicle pinches off, and Sec2p activates Sec4p, which then recruits its effector, Sec15p. Before delivery of the vesicle to the plasma membrane, the level of PI(4)P decreases, triggering a conformation change in Sec2p, which allows Sec15p to replace Ypt32p-GTP on Sec2p. Sec2p undergoes phosphorylation that enhances the interaction of Sec2p with Sec15p and inhibits binding to Ypt32p-GTP and PI(4)P, pushing the reaction forward. This process creates a positive-feedback loop because the GEF Sec2p is able to bind directly to an effector of the activated Rab Sec4p. Thus, a microdomain of high Sec4p-GTP and high effector concentration is generated, facilitating the delivery, tethering, and fusion of the vesicle with the plasma membrane. Sec2p then is dephosphorylated, triggering its release from Sec15p and allowing Sec2p to associate with a new round of secretory vesicles, thus ensuring the continuity of vesicular transport.

phosphorylated by the cyclin-dependent kinase Cdc28p, but the site of phosphorylation is close to the C terminus, at serine 584, rather than within the Ypt32p/Sec15p-binding region (21). It will be important to identify and localize the kinase that phosphorylates Sec2p in vivo as well as the competing phosphatase. Defining the spatial and temporal regulation of Sec2p phosphorylation should yield important insights into its function.

Materials and Methods

Plasmid Construction and Strains. To generate the various GST-Sec2 mutants, PCR-based site-directed mutagenesis of the pGEX4T1-Sec2 (NRB1152) vector was performed. Phosphosites were mutated to an alanine to mimic the unphosphorylated state and to an aspartic acid (for serines) or a glutamic acid (for threonines) to mimic the phosphorylated state. After sequencing to confirm the presence of the mutation, the plasmid was used for expression in *Escherichia coli*.

The same strategy was used to mutagenize the pRS305-Sec2-3×GFP (NRB1416) integrating yeast vector. The mutant plasmids then were linearized using NsiI and were transformed into yeast (NY1210) at the *SEC2* locus. Sequence analysis was performed to confirm that the changes in the *sec2* mutants had integrated into the sole full-length copy in the genome. Yeast strains with the *ypt31*Δ *ypt32*^{A141D} mutations or coexpressing Sec15p-13×myc were made by crossing the *sec2* mutant strains to MY481 or NY2545, respectively.

To express GST-Sec2p mutants (S181–8A and S181–8D/E) in yeast, Sec2 fragments bearing the mutations were excised from pGEX4T1-Sec2 vectors with NsI1 and NdeI and were cloned back into the Gal-inducible vector pNB529-GST-Sec2. pNB529-GST-Sec2, linearized with ClaI, then was introduced into the protease-deficient *pep4::HIS3* yeast strain NY603. For a list of yeast strains used in this study, see Table S1. For a list of plasmids, see Tables S2 and S3.

Expression and Purification of GST Sec2p and His$_6$-Tagged Sec15p and Ypt32p in *E. coli*. GST-Sec2p in pGEX4T1 was transformed into *E. coli* Bl21 cells. Cells were grown at 37 °C to an OD_{600} of 0.6 and were induced using 0.1 mM isopropyl β-D-1-thiogalactopyranoside overnight at 16 °C. The bacterial pellet was resuspended in 1× PBS, 5 mM $MgCl_2$, 1 mM PMSF, protease inhibitors (Complete EDTA-free protease inhibitor mixture tablets from Roche), and 1 mM DTT. Cells were disrupted by sonication, and Triton X-100 was added to the suspension to a final concentration of 1% followed by 15-min incubation at 4 °C. The suspension then was cleared by centrifugation (27,000 × *g* for 30 min at 4 °C). After 60-min incubation with glutathione-Sepharose beads (GE Healthcare), the beads were washed with 1× PBS, 1 mM $MgCl_2$, 0.1% Triton X-100, and 1 mM DTT and were used for in vitro binding experiments the following day.

For sedimentation experiments, GST-Sec2p was eluted with a buffer containing 100 mM Tris (pH 8.0), 300 mM NaCl, and 20 mM glutathione. Glutathione then was removed by dialysis against 20 mM Tris (pH 7.2), 100 mM NaCl, 1 mM $MgCl_2$, 1 mM DTT, and 10% (vol/vol) glycerol.

His$_6$-Sec15p and His$_6$-Ypt32p were expressed and purified from *E. coli* Rosetta 2 cells as described previously (15). After elution with imidazole, His$_6$-Sec15p and His$_6$-Ypt32p were dialyzed as described above for GST-Sec2p.

The concentration of purified protein was determined by SDS/PAGE with BSA as standard.

Expression, Purification, and CIP Treatment of GST-Sec2p from Yeast. Two hundred OD_{600} units of yeast overexpressing GST-Sec2p (NY2948, NY2949, NY3031, NY3032) was resuspended in lysis buffer containing 1× PBS, 1 mM $MgCl_2$, 1 mM PMSF, protease inhibitors (Complete EDTA-free protease inhibitor mixture tablets from Roche), and 5 mM DTT. Cells were disrupted in a bead beater using 0.5-mm zirconia/silica beads. Triton X-100 was added to the lysate to a final concentration of 1% followed by a 15-min incubation at 4 °C and finally the lysate was cleared by centrifugation at 18,000 × *g* for 20 min. Supernatants then were incubated with 200 μL of glutathione-Sepharose beads for 2 h at 4 °C. After the incubation, the beads were washed three times with 1 mL of a buffer containing 1× PBS, 1 mM $MgCl_2$, 0.5% Triton X-100, and 1 mM DTT.

For CIP treatment, the beads were washed three times with 0.5 mL of NEB buffer 3 (New England Biolabs) and were incubated with CIP for 1 h at 37 °C [5 μL of CIP enzyme (10,000 U/mL) from New England Biolabs in 200 μL of a 50% slurry of beads].

In Vitro Binding Assay. His$_6$-Ypt32p was preloaded with GTPγS (Roche) in a buffer containing 1× PBS, 1 mM nucleotide, 1 mg/mL BSA, 1 mM EDTA, and 1 mM DTT for 1 h at room temperature. Then 5 mM $MgCl_2$ was added to the reaction, and it was incubated for another 30 min.

GST or GST-Sec2p (2.5 μg) immobilized on glutathione-Sepharose beads (purified the previous day and stored at 4 °C overnight) was incubated with His$_6$-Ypt32p (0.6 μM) in 1× PBS, 0.5 mg/mL BSA, 0.5 mM $MgCl_2$, 0.1 mM nucleotide, 0.025% Triton X-100, and 0.5 mM DTT. The total volume of incubation mixtures was 200 μL. After 1 h incubation at 4 °C, the beads were washed three times with a buffer (500 μL) containing 1× PBS, 5 mM $MgCl_2$, 10 μM nucleotide, 0.05% Triton X-100, and 1 mM DTT. Bound products were separated by SDS/PAGE and analyzed with anti-Ypt32 antibody (1:6,000 dilution) (a gift from the Ferro-Novick laboratory, University of California, San Diego, La Jolla, CA) as the primary antibody. The amount of GST-Sec2p in the reaction was verified by Western blotting with anti-GST antibody (1:1,000 dilution; sc-459; Santa Cruz Biotechnology). HRP-conjugated goat anti-rabbit IgG (1:10,000 dilution) was used as the secondary antibody and was detected with Pierce ECL Western Blotting Substrate (Thermo Scientific).

The binding of His$_6$-Sec15p to GST alone or to GST-Sec2p immobilized on glutathione-Sepharose beads was conducted in a similar manner except that only 0.5 μg of His$_6$-Sec15p was used, the binding reaction was free of both nuceotide and Triton X-100, and the wash buffer was nucleotide free. Bound products were analyzed with anti-Sec15 antibody (1:2,000 dilution) as the primary antibody.

Immunoprecipitation Assay. Yeast cells were grown overnight to midlog phase in a YPD medium at 25 °C. Seventy-five OD_{600} units of cells were collected and washed with 10 mM NaN3 and 1.2 M sorbitol. Cells were resuspended with 1% 2-mercaptoethanol in 50 mM Tris (pH 8.0) and were incubated for 10 min at 30 °C. Cells were spheroplasted in a potassium phosphate buffer (pH 7.5) containing 1.2 M sorbitol, 1 mM $MgCl_2$, and 24 μg/μL of lyticase for 1 h at 30 °C with gentle shaking. Spheroplasts were pelleted (500 × *g* for 5 min at 4 °C) and washed twice with ice-cold 1.2 M sorbitol. Lysis was performed with a glass homogenizer in the following buffer: 10 mM triethanolamine-AcOH (pH 7.2), 0.4 M sorbitol, 1 mM EDTA, 5 mM PMSF, and protease inhibitors. Then 1% of Triton X-100 was added to the lysates. After incubation at 4 °C for 15 min, lysates were centrifuged at 18,000 × *g* for 20 min. The total protein concentration in the supernatant was measured by Bradford protein assay (Bio-Rad Laboratories). Lysates were precleared with 10 μL of protein A/G beads (Thermo Scientific) for 60 min at 4 °C. Sec2-3×GFP was immunoprecipitated overnight at 4 °C with purified anti-GFP polyclonal antibody (a gift from the Ferro-Novick laboratory). Then 10 μL of protein A/G

beads was added and incubated for 2 h at 4 °C. Beads were washed four times with 1 mL PBS1× buffer. Immunoprecipitates were analyzed with Western blotting with anti-Myc antibody (1:1,000 dilution; 9B11 mouse; Cell Signaling Technology) and anti-GFP antibody (1:1,000). HRP-conjugated goat anti-mouse or anti-rabbit IgG (1:10,000 dilution) was used as the secondary antibody and was detected with Pierce ECL Western Blotting Substrate (Thermo Scientific).

Liposome Preparation. 1-Palmitoyl-2-oleoyl-sn-glycero-3-phospho-L-serine (POPS), 1,2-dipalmitoyl-sn-glycero-3-phosphoethanolamine (DPPE), 1,2-dipalmitoyl-sn-glycero-3-phosphocholine (DPPC), and brain PI(4)P were from Avanti Polar Lipids. All liposomes contained 20 mol% DPPE and 30 mol% POPS, with or without 5 mol% PI(4)P. The remaining lipid was DPPC. Lipids in chloroform were mixed in a pear-shaped glass container. The glass container was attached to a rotary evaporator and immersed in a water bath at 33 °C for 5 min before evaporation. A lipid film was produced by rapid evaporation of chloroform under vacuum. The lipid film was resuspended in 50 mM Hepes, 210 mM Sucrose, pH 7.2 (4 mM lipids). The resuspension was submitted to five cycles of freezing and thawing and was extruded through a polycarbonate filter with a pore size of 0.1 μm.

Sedimentation Experiment. GST-Sec2p (0.4 μM) was incubated with 0.4 mM extruded sucrose-loaded, liposomes in a buffer containing 50 mM Hepes, 120 mM potassium acetate, 1 mM $MgCl_2$, 1 mM DTT, pH 7.2. The volume of the mix was 70 μL. After 15 min at room temperature, the suspension was centrifuged at 55,000 rpm for 15 min at 25 °C in a TLA 120.2 rotor. The lipid pellet was resuspended in the same volume of buffer. Proteins in the pellet and in the supernatant were visualized by Coomassie Brilliant Blue staining after SDS/PAGE. The intensity of the bands was analyzed with ImageJ.

Limited Proteolysis. About 2.5 μg of GST-Sec2p proteins, purified from bacteria or from yeast and treated with the phosphatase CIP or left untreated, was subjected to trypsin digestion as described previously (14).

Growth Test. Cells were grown overnight in YPD medium at 25 °C. Cells were diluted to an OD_{600} of 0.04 and spotted in fivefold serial dilution on YPD plates which were incubated at different temperatures.

Fluorescence Microscopy. For GFP visualization, yeast cells were grown overnight to midlog phase in a synthetic medium containing 2% glucose at 25 °C. Live cells (500 μL) were pelleted by centrifugation at 13,000 rpm for 1 min and were resuspended in 50 μL of medium. Then 5 μL of the cell suspension was spotted on a glass slide. Fluorescence images were acquired with a 100× oil immersion objective on a Yokagawa spinning-disk confocal microscopy system (Zeiss Carl Observer Z.1) equipped with an electron multiplying CCD camera (QuantEM 512SC; Photometrics), and excitation of GFP was achieved using a 488-nm argon laser. For each sample, a z-stack with a 300-nm slice distance was generated. Images were analyzed using AxioVision software 4.8. Sec2p localization was quantified based on polarized localization in unbudded cells, at the tips of small/medium budded cells, and at the mother–daughter necks of larger cells. About 150 cells were examined for each condition, and at least three separate experiments were used to calculate the SD.

Electron Microscopy. Yeast cells expressing wild-type Sec2 or Sec2-S181–8A fused to 3×GFP in the wild-type background (NY2911 and NY3037) or in the *ypt31*Δ *ypt32*^{A141D} background (NY3040 and NY3045) were grown at 25 °C in YPD medium, were shifted to 32 °C for 1 h, and were processed for electron microscopy as described by Chen et al. (22).

Mass Spectrometry. GST-Sec2p 1–508 (NY2436) was purified from yeast. About 2 μg of purified protein was loaded on an SDS/PAGE gel; then the band was cut out and subjected to trypsin digestion as described in ref. 23.

Trypsin-digested peptides were analyzed by HPLC coupled with LC-MS/MS using nano-spray ionization. The nanospray ionization experiments were performed using a TripleTof 5600 hybrid mass spectrometer (ABSCIEX) interfaced with nano-scale reversed-phase HPLC (Tempo) using a 10-cm glass capillary (100 μm i.d.) packed with 5-μm C18 Zorbax beads (Agilent Technologies). Peptides were eluted from the C18 column into the mass spectrometer using a linear gradient (5–60%) of acetonitrile (ACN) at a flow rate of 250 μL/min for 1 h. The buffers used to create the ACN gradient were 98% H_2O, 2% ACN, 0.2% formic acid, and 0.005% TFA (buffer A) and 100% ACN, 0.2% formic acid, and 0.005% TFA (buffer B). MS/MS data were acquired in a data-dependent manner in which the MS1 data were acquired for 250 ms at *m/z* of 400–1,250 Da and the MS/MS data were acquired from *m/z* of 50–2,000 Da. For independent data acquisition (IDA) the parameters were MS1-TOF 250 ms, followed by 50 MS2 events of 25 ms each. The independent data acquisition (IDA) parameters were set to trigger MS2 events when the parent ion of plus 2-4 charge state, showed an intensity level of over 200 counts. The exclusion time for the selected ions was set to 4 s. Finally, the collected data were analyzed using MASCOT (Matrix Sciences) and Protein Pilot 4.0 (ABSCIEX) for peptide identifications.

ACKNOWLEDGMENTS. We thank Ying Jones from M. Farquhar's laboratory for the preparation of samples for electron microscopy, Deepali Bhandari from M. Farquhar's laboratory for helpful discussions, Juan Wang from S. Ferro-Novick's laboratory for the gift of purified anti-GFP antibody, S. Ferro-Novick's laboratory for anti-Ypt32 antibody, and S. Dowdy's laboratory for allowing us to use their rotary evaporator, all at the University of California, San Diego. This study was supported by the National Institutes of Health Grant GM82861 (to P.J.N.). D.S. was supported by Swiss National Science Foundation Grants PBSKP3_138593 and PBSKP3_145803.

1. Hutagalung AH, Novick PJ (2011) Role of Rab GTPases in membrane traffic and cell physiology. *Physiol Rev* 91(1):119–149.
2. Cherfils J, Zeghouf M (2013) Regulation of small GTPases by GEFs, GAPs, and GDIs. *Physiol Rev* 93(1):269–309.
3. Jin Y, et al. (2011) Myosin V transports secretory vesicles via a Rab GTPase cascade and interaction with the exocyst complex. *Dev Cell* 21(6):1156–1170.
4. Guo W, Roth D, Walch-Solimena C, Novick P (1999) The exocyst is an effector for Sec4p, targeting secretory vesicles to sites of exocytosis. *EMBO J* 18(4):1071–1080.
5. Grosshans BL, et al. (2006) The yeast lgl family member Sro7p is an effector of the secretory Rab GTPase Sec4p. *J Cell Biol* 172(1):55–66.
6. Walch-Solimena C, Collins RN, Novick PJ (1997) Sec2p mediates nucleotide exchange on Sec4p and is involved in polarized delivery of post-Golgi vesicles. *J Cell Biol* 137(7): 1495–1509.
7. Dong G, Medkova M, Novick P, Reinisch KM (2007) A catalytic coiled coil: Structural insights into the activation of the Rab GTPase Sec4p by Sec2p. *Mol Cell* 25(3):455–462.
8. Elkind NB, Walch-Solimena C, Novick PJ (2000) The role of the COOH terminus of Sec2p in the transport of post-Golgi vesicles. *J Cell Biol* 149(1):95–110.
9. Ortiz D, Medkova M, Walch-Solimena C, Novick P (2002) Ypt32 recruits the Sec4p guanine nucleotide exchange factor, Sec2p, to secretory vesicles; evidence for a Rab cascade in yeast. *J Cell Biol* 157(6):1005–1015.
10. Knödler A, et al. (2010) Coordination of Rab8 and Rab11 in primary ciliogenesis. *Proc Natl Acad Sci USA* 107(14):6346–6351.
11. Mizuno-Yamasaki E, Rivera-Molina F, Novick P (2012) GTPase networks in membrane traffic. *Annu Rev Biochem* 81:637–659.
12. Pusapati GV, Luchetti G, Pfeffer SR (2012) Ric1-Rgp1 complex is a guanine nucleotide exchange factor for the late Golgi Rab6A GTPase and an effector of the medial Golgi Rab33B GTPase. *J Biol Chem* 287(50):42129–42137.
13. Nottingham RM, et al. (2012) RUTBC2 protein, a Rab9A effector and GTPase-activating protein for Rab36. *J Biol Chem* 287(27):22740–22748.
14. Medkova M, France YE, Coleman J, Novick P (2006) The rab exchange factor Sec2p reversibly associates with the exocyst. *Mol Biol Cell* 17(6):2757–2769.
15. Mizuno-Yamasaki E, Medkova M, Coleman J, Novick P (2010) Phosphatidylinositol 4-phosphate controls both membrane recruitment and a regulatory switch of the Rab GEF Sec2p. *Dev Cell* 18(5):828–840.
16. Chiba S, Amagai Y, Homma Y, Fukuda M, Mizuno K (2013) NDR2-mediated Rabin8 phosphorylation is crucial for ciliogenesis by switching binding specificity from phosphatidylserine to Sec15. *EMBO J* 32(6):874–885.
17. Ultanir SK, et al. (2012) Chemical genetic identification of NDR1/2 kinase substrates AAK1 and Rabin8 Uncovers their roles in dendrite arborization and spine development. *Neuron* 73(6):1127–1142.
18. Jedd G, Mulholland J, Segev N (1997) Two new Ypt GTPases are required for exit from the yeast. *J Cell Biol* 137(3):563–580.
19. Cabrera M, et al. (2010) Phosphorylation of a membrane curvature-sensing motif switches function of the HOPS subunit Vps41 in membrane tethering. *J Cell Biol* 191(4):845–859.
20. Kurischko C, et al. (2008) The yeast LATS/Ndr kinase Cbk1 regulates growth via Golgi-dependent glycosylation and secretion. *Mol Biol Cell* 19(12):5559–5578.
21. Bishop A, et al. (2010) Hyphal growth in Candida albicans requires the phosphorylation of Sec2 by the Cdc28-Ccn1/Hgc1 kinase. *EMBO J* 29(17):2930–2942.
22. Chen S, Novick P, Ferro-Novick S (2012) ER network formation requires a balance of the dynamin-like GTPase Sey1p and the Lunapark family member Lnp1p. *Nat Cell Biol* 14(7):707–716.
23. Shevchenko A, Wilm M, Vorm O, Mann M (1996) Mass spectrometric sequencing of proteins silver-stained polyacrylamide gels. *Anal Chem* 68(5):850–858.